Preparation of High-Modulus Poly(ethylene terephthalate) Fibers by Vibrating Hot Drawing

TOSHIO KUNUGI* and AKIHIRO SUZUKI

Department of Applied Chemistry and Biotechnology, Faculty of Engineering, Yamanashi University, 4-3-11 Takeda, Kofu 400 Japan

SYNOPSIS

A novel drawing method, vibrating hot drawing, was successfully applied to poly(ethylene terephthalate) fiber, which has a normal molecular weight (IV = 0.7 dL/g) and was prepared by melt spinning. The process was divided into three steps, with differing conditions in drawing temperature, applied tension, vibrating frequency, and amplitude. The drawing temperature and vibration frequency were decided by considering the α_a dispersion of the polymer. In spite of a low draw ratio (7.7) and a low crystallinity (0.55), the birefringence and dynamic storage modulus at room temperature of the 3rd-step fiber reached 0.260 and 36 GPa, respectively. The modulus remains at a high level at elevated temperatures, for example, 29 GPa at 100°C and 17 GPa at 200°C. Further, it was found from temperature and intensity of the α_a dispersion peak that the movements of amorphous chains are strongly inhibited. © 1996 John Wiley & Sons, Inc.

INTRODUCTION

In order to improve mechanical properties of an important commercial fiber, poly(ethylene terephthalate) (PET), a variety of spinning, drawing, and annealing methods[1-15] have been proposed. In Table I, the main methods are listed in the order of the publications with the chief researchers and the maximum values of modulus (E) and tensile strength (σ).

The moduli of polyethylene[16] and poly(vinyl alcohol)[17] reached at fairly high levels, namely 232 GPa and 115 GPa, which are 96 and 46% of the crystal moduli along molecular chains of 235 and 250 GPa, respectively. However, the maximum modulus[15] of PET fiber is only 39 GPa, corresponding to 36.1% of the crystal modulus, 108 GPa.

In order to overcome this situation, other novel routes to high modulus have been strongly desired. We have succeeded in developing a novel drawing method, vibrating hot-drawing method.[18] So far, this method has been applied to semicrystalline polymer fibers such as PET,[18] Nylon 6,[19,20] and poly(vinyl alcohol),[19,21] polyarylate[22] fibers. In all cases, the

mechanical properties had been remarkably improved.

The present article deals with the application of the vibrating hot-drawing method to a commercial grade PET fiber. In spite of the simple apparatus and easy procedure, the dynamic storage modulus at room temperature reached 36 GPa.

EXPERIMENTAL

Material

The original material was an as-spun, undrawn, and almost-amorphous fiber of 248 μm diameter, supplied by Toray Co. Ltd. The fiber has a crystallinity of 0.01, a birefringence of 1×10^{-4}, and an intrinsic viscosity of 0.7 dL/g. From DSC curve, it was found that T_g, cold-crystallization temperature, and melting point are 77.3°C, 127.6°C, and a double peak of 243.5 and 253.3°C, respectively.

Vibrating Hot Drawing

Figure 1 shows a scheme of apparatus used for the vibrating hot drawing. The apparatus is constituted of an amplifier, a vibrator equipped with an accel-

---

Table I   Various Drawing, Annealing, and Spinning Methods for PET Fibers or Films

Year	Method	Chief Researchers	E (GPa)	σ (GPa)	Ref.
1981	Zone-drawing/zone-annealing	Kunugi	19.4	0.8	1
1983	Solid-state coextrusion	Porter	11	0.4	2
1984	Cold drawing/annealing under a high tension	Kitao	26	0.6	3
1986	High-speed melt-spinning/ hot-drawing	Yoon	17.4	1.1	4
1987	Solid-state coextrusion/two-step drawing of cast film	Kanamoto	17.5	0.4	5
1987	Microwave heat-drawing	Nakagawa	25.0	—	6
1988	Cold-drawing/long-time annealing of cast film	Itoyama	35.4	—	7
1990	Solid-state polymerization/ solution-spinning/drawing	Kanamoto	34.4	1.9	8
1990	Drawing at RT/annealing under constant strain	Fakirov	18.6	0.6	9
1991	High-speed melt-spinning/pin and plate drawing	Ward	17.5	0.97	10
1991	Zone-drawing/annealing under extremely-high tension	Kunugi	30	1.7	11
1991	Production by Allied-Signal Co.	Rim	13.5	1.1	12
1992	Multistage combined drawing/ zone-drawing	Goschel	16.8	—	13
1992	Solid-state polymerization/two-stage drawing	Ito	23.8	1.5	14
1994	High molecular weight PET/ solution-spinning/three-stage drawing	Kanamoto	39	2.3	15

erometer, and an electric furnace. One end of the fiber was fixed at the vibrator head, and another end was attached to a dead weight so that a suitable tension occurs. The fiber was heated in the electric furnace at a desired temperature. The vibration frequency (f) can be selected in the range from 2 to 20,000 Hz. Also, the optimum amplitude (D) or acceleration (A) was selected. The relation between these factors is represented by the following equation

$$D = 980A/(2\pi f)^2 \qquad (1)$$

The conditions for the vibrating hot drawing are the drawing temperature, applied tension, vibration frequency, and amplitude. The process was divided into three steps; the 1st step was done with a view to orienting the molecular chains and inhibiting the crystallization. The 2nd step was carried out with the intention of extension of the oriented amorphous chains at the same temperature under a higher tension. The 3rd step was carried out with the objects of further extension of amorphous chains and of

formation of the extended-chain crystals at a suitable crystallization temperature under a very high tension.

After a number of preliminary experiments, the conditions shown in Table II were decided. The treatment time was 10 min for each step.

Measurements

The birefringence (Δ_t) was measured with a polarizing microscope equipped with a Berec compensator. As an additional compensator, X-Z planes of various thicknesses cut from a single crystal of quartz were used on the measurements. The orientation factor of crystallites (f_c) was evaluated by the x-ray diffraction method. The f_c is defined by $f_c = \frac{1}{2}(3\langle\cos^2\Phi_{c,z}\rangle - 1)$, where $\langle\cos^2\Phi_{c,z}\rangle$ represents the mean-square cosine of the angle between the c axis and the fiber axis (z), and can be calculated by the following equation derived from an application of the Wilchinsky's method.
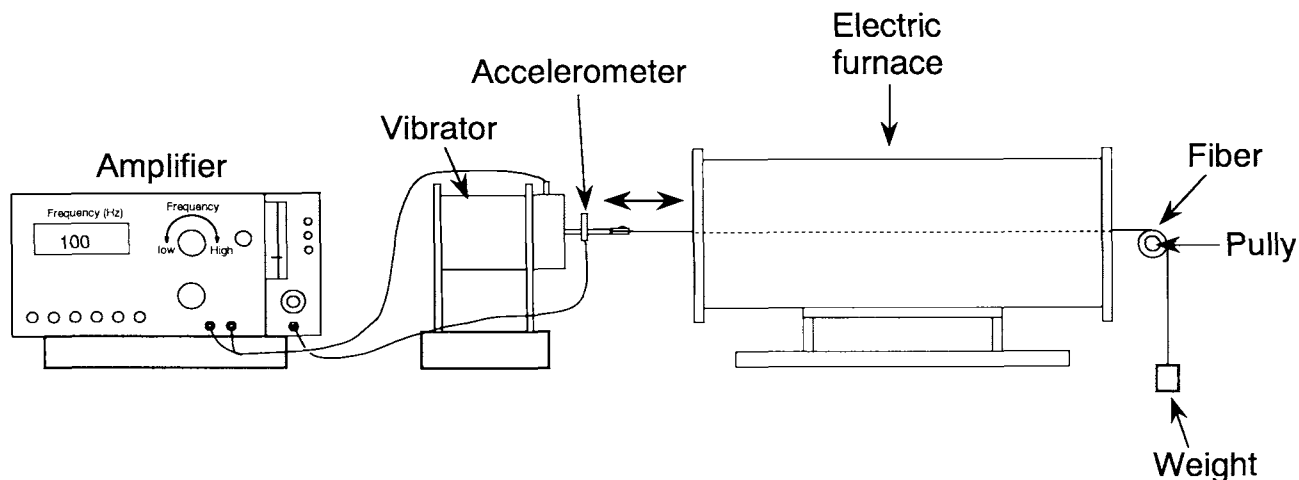
Figure 1   Scheme of apparatus used for the vibrating hot-drawing method.

$$\langle \cos^2\Phi_{c,z} \rangle = 1 - 0.3481\langle \cos^2\Phi_{100,z} \rangle - 0.7733$$

$$\langle \cos^2\Phi_{\bar{1}10,z} \rangle - 0.8786\langle \cos^2\Phi_{010,z} \rangle \quad (2)$$

where the quantities $\langle \cos^2\Phi_{100,z} \rangle$, $\langle \cos^2\Phi_{\bar{1}10,z} \rangle$, and $\langle \cos^2\Phi_{010,z} \rangle$ can be graphically determined from the azimuthal intensity distributions of x-ray diffraction for the (100), ($\bar{1}$10), and (010) planes, respectively.

Also, the orientation factor of amorphous chains (f_a) was calculated by substituting the f_c, crystallinity (X), and the intrinsic birefringences of the crystallites and amorphous chains (Δ_c and Δ_a) into the following equation.

$$f_a = (\Delta_t - X \cdot f_c \cdot \Delta_c)/(1 - X)\Delta_a \quad (3)$$

The procedure was described in detail in the previous article.[1]

The density was measured at 25°C by a flotation method using toluene–carbon tetrachloride mixtures. From the obtained density, the X was calculated by the usual method using a crystal density[23] of 1.455 g/cm³ and an amorphous density[23] of 1.335 g/cm³. The dynamic viscoelastic properties, E', E'', and tan δ, were measured at 110 Hz at a heating rate of 1.5°C/min on 20 mm-long fibers over a tem-

perature range from room temperature to 220°C with a dynamic viscoelastometer, VIBRON DDV-II (Orientec Co., Ltd.).

RESULTS AND DISCUSSION

Principle and Characteristics of Vibrating Hot-Drawing Method

The mechanical properties of semicrystalline polymer fibers depend strongly on the superstructure of amorphous regions. Generally, the amorphous chains are not fully oriented and extended after drawing. In the usual drawing methods, the drawing force is concentrated on the weak point of the structure resulting in a breakage of the fiber, and is not effectively used for formation of a homogeneously stretched chain structure.

Then the vibrating hot-drawing method, in which the fibers are hot drawn under vibration, was proposed. It was expected that the vibration may draw out molecular chains in cooperation with heating and tension from a complicated structure, weakening intermolecular forces such as chain entanglements, hydrogen bonds, or steric hindrances. The heating

Table II   Conditions for Vibrating Hot Drawing

Step	Drawing Temperature (°C)	Applied Tension (kg/mm²)	Frequency (Hz)	Amplitude (μm)
1st	90	1	100	100
2nd	90	21	10	120
3rd	220	24	10	120

Original fiber   1st step fiber   2nd step fiber   3rd step fiber
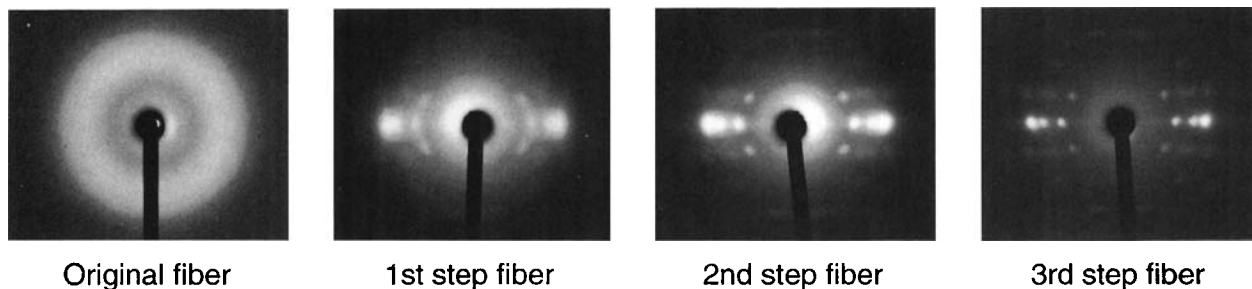
Figure 2   Wide-angular x-ray diffraction photographs for the original, 1st-step, 2nd-step, and 3rd-step fibers.

also is useful to weaken the intermolecular forces and to facilitate the movement of molecular chains. Because the vibration is in the same direction as the drawing direction, the applied tension inhibits the orientation relaxation and cumulates the displacement.

Also, when the vibration head moves in the reverse of the tension direction, a high stress generates. Such a high stress occurs momentarily, but is repeated numerous times. So the fiber structure easily approaches a limiting structure attainable under the given conditions. When the drawing takes place, the vibration of the fiber is remarkably diminished. The vibration energy is consumed for a plastic flow of molecular segments.

Determination of Optimum Conditions for Vibrating Hot Drawing

When the drawing temperature rises from a temperature fully below T_g at a constant frequency and under a constant tension, the draw ratio is suddenly increased at a temperature near to the α_a dispersion temperature of the polymer. It is clear from this that the α_a dispersion gives a clue of the determination of conditions for vibrating hot drawing. The α_a dispersion is attributed to micro-Brownian motions of molecular segments in the amorphous regions. In this temperature range, the E' is clearly decreased and the corresponding dispersion peak appears in temperature–E'' or –tan δ curves. The α_a dispersion peak, as well as γ, β, and α_a dispersion peaks, occurs at a defined set of frequency and temperature. As the used frequency increases within the permissible range, the dispersion peak shifts to a higher temperature. The relation between the frequency (f) and the peak temperature (T_p) is represented by a dispersion map (log f vs. $1/T_p$) drawn in the form of a straight line for each dispersion. From the slope of straight line, an apparent activation energy (ΔH_a)

for the dispersion can be calculated by the use of the following equation:

$$\Delta H_a = 2.303Rd \log f/d(1/T_p) \qquad (4)$$

where R is gas constant. Further, the dispersion peak is formed at $\omega\tau = 1$ or log $\omega\tau = 0$, where ω is a circular frequency and τ is a relaxation time. The ω is related to the f by $\omega = 2\pi f$. On the basis of above criterion, the conditions were roughly decided. As seen in Table II, the drawing temperature of 90°C used at the 1st and 2nd steps is reasonable in this point. The frequency decreased from 100 Hz at 1st step to 10 Hz at the 2nd step. The fiber structure after 1st step becomes harder due to molecular orientation and orientation crystallization. So the τ must be longer, namely, the smaller frequency should be used. The 3rd vibrating hot drawing was performed at 220°C. Because the fiber becomes soft at higher temperatures, the τ becomes smaller. However, the fiber structure becomes hard by the 1st and 2nd processes. Consequently, the frequency of 10 Hz was used again at the 3rd step. The objects of the 3rd step, as described above, is the extension of yet unstretched amorphous chains and of the crystallization of highly oriented amorphous chains. Therefore, the high tension and high temperature were used. It can be considered that PET is an especially favorable material for the vibrating hot-drawing method, because the original fiber is almost amorphous.

Superstructure

Figure 2 shows wide angular x-ray diffraction photographs for the original, 1st-step, 2nd-step, and 3rd-step fibers. It is qualitatively found that the crystallite orientation and crystallinity increase with the processes. To examine in more detail, the changes

Table III Draw Ratio (DR), Birefringence (Δ_t), Orientatio Factors of Crystallites and Amorphous Chains (f_c and f_a) and Crystallinity (X) for Each Step Fiber

Step	DR	Δ_t	f_c	f_a	X
Original	1.0	—	—	—	0.01
1st	4.1	0.191	—	—	0.33
2nd	5.7	0.222	—	—	0.34
3rd	7.7	0.260	0.981	0.749	0.55
3rd (without vibration)	6.4	0.245	0.983	0.668	0.51

in draw ratio (DR), Δ_t, f_c, f_a, and X are shown in Table III.

Although the DR increased step by step, the attained maximum DR is only 7.7. In most of the studies listed in Table I, the DR values are in the range of 4–9. The values above DR 10 were obtained by Fakirov et al.,[9] 20, and by Kanamoto et al.,[15] 16.4. As well known, the drawability of original fibers depends on an initial morphology, molecular weight, and drawing method. Fakirov et al. and Kanamoto et al. used the high molecular weight PET (2.6 dL/ g) obtained by solid-state polymerization, whereas the original fiber used in the present study is an as-spun fiber with a commercially available molecular weight (0.7 dL/g). This may be one of reasons of such a low DR.

However, the Δ_t value of the 3rd-step fiber is 0.260, which is remarkably high and is higher than Δ_c(0.251) estimated by us.[24] This value also is identical to the values obtained by Gupta et al.[25] and Nakagawa et al.[6] We recently obtained a still higher Δ_t value of 0.276 by a novel drawing method, "Extremely high tension annealing method."[26]

The highest X value for PET in the literature is 0.90 by Itoyama.[7] The film was prepared by tensile drawing to 4.3 times at 25°C and annealing at 260°C during 360 h under a constant length of 1.25 times. In general, the high X value can be obtained by the long time annealing. Compared with this, the X of the 3rd-step fiber is only 0.55. Although the crystallization was avoided at 1st and 2nd step, the X of the resulting fibers are 0.33 and 0.34. In spite of a very large tension of 21 kg/mm² at the 2nd step, X almost did not increase. It seems to be a limit of crystallinity on the vibrating drawing at 90°C. However, the X reached 0.55 by the 3rd-step vibrating hot drawing at 220°C under 24 kg/mm².

The f_c of the 1st- and 2nd-step fibers could not be evaluated, because x-ray diffraction peaks for (100), ($\bar{1}$10), and (010) planes could not separated, owing to overlap of these peaks.

The f_a can be calculated by eq. (2). The combinations of Δ_c and Δ_a have been so far proposed by many researchers. Now the f_a was calculated by substituting several combinations[24,25,27-30] of Δ_c and Δ_a for the 3rd-step fiber having $\Delta_t = 0.260$, $X = 0.55$, and $f_c = 0.981$. The results are shown in Table IV. All f_a values, except 0.749, are estimated beyond unity, which cannot be accepted as f_a. The combination of 0.310 and 0.275 proposed by Gupta et al.[25] alone provided a reasonable value of 0.749. This fact suggests an important problem for the orientation evaluation of semicrystalline polymers. It is required at least that:

$$\Delta_c \leq \Delta_t/(X \cdot f_c) \quad \text{and}$$

$$\Delta_a \geq (\Delta_t - X \cdot f_c \cdot \Delta_c)/(1 - X) \quad (5)$$

should hold simultaneously on the basis of the limitations of $0 \leq f_a \leq 1$ and $0 \leq X \leq 1$, which are necessary but not sufficient conditions. However, there are still questions about eq. (3) and the two-phase model.

In order to check the effect of vibration, the data for the 3rd-step fiber, was prepared without vibration show in Table III. The DR, Δ_t, and X are slightly lower than those of the 3rd-step fiber. The f_a is especially very low in the case of hot drawing without

Table IV Values of f_a Calculated Using Various Combinations of Δ_c and Δ_a for the 3rd-Step Fiber Having $\Delta_t = 0.260$, $X = 0.55$, and $f_c = 0.981$
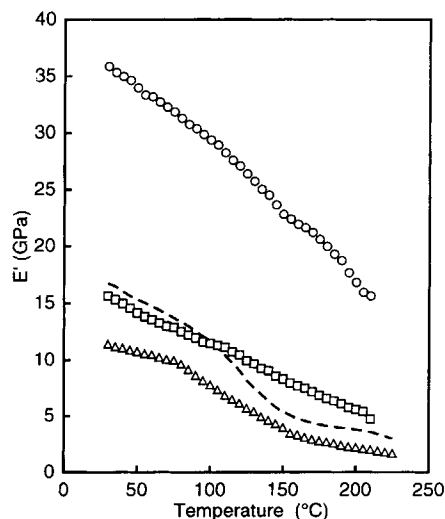
Researcher	Δ_c	Δ_a	f_a	Ref.
DeVries	0.220	0.20	1.57	27
Kunugi	0.251	0.230	1.204	24
Gupta	0.290	0.20	1.150	28
Dumbleton	0.220	0.275	1.142	29
Heuvel	0.220	0.240	1.308	30
Gupta	0.310	0.275	0.749	25

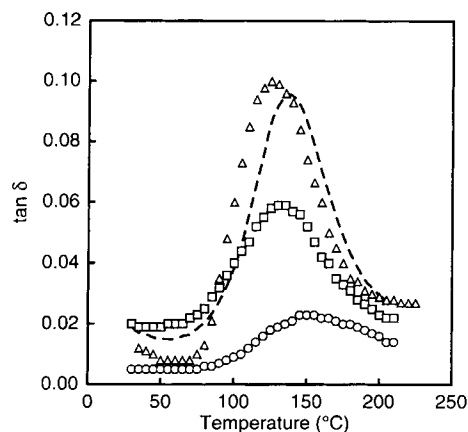vibration. In other words, it can be said that the vibration is very useful to orient the amorphous chains.

Dynamic Viscoelastic Properties

Figure 3 shows the temperature dependence of E' for the 1st-, 2nd-, and 3rd-step fibers and the 3rd-step fiber prepared without vibration. The E' is remarkably increased stepwise; particularly, the increment of E' by the 3rd step is striking. It reached 36 GPa at room temperature, which is about twice that of the 3rd-step fiber prepared without vibration. Further, the E' value remains at a high level at elevated temperatures, for example, 29 GPa at 100°C and 17 GPa at 200°C. Compared with the data indicated in Table I, the value is lower by 3 GPa than 39 GPa reported by Kanamoto et al.,[15] but is comparable to 35.4 GPa by Itoyama.[7] Kanamoto et al.[15] used the high molecular weight PET (IV = 2.41), and a process that consists of a solution spinning and three step drawings at 8, 90, and 200°C. Itoyama[7] used PET with M_n = 380,000 and a process that consists of a casting, cold drawing at 25°C, and annealing at 260°C for 360 h. In comparison with these processes, the method in the present study has characteristics using a general molecular weight PET (IV = 0.7), and a nonsolvent, simple, and easy processing.

Figure 4 shows the temperature dependence of tan δ for the 1st-, 2nd-, and 3rd-step fibers and the 3rd-step fiber prepared without vibration. The α_a

Figure 4 Temperature dependence of tan δ; 1st-step, fiber ($\triangle$), 2nd-step fiber ($\bigcirc$), 3rd-step, fiber ($\square$), and the 3rd-step fiber prepared without vibration (-----).

dispersion peak shifts to higher temperatures and decreases in height in order of the 1st, 2nd, and 3rd steps. The peak temperature shifts from 125°C for the 1st-step fiber to 155°C for the 3rd-step fiber being higher by 15°C than 140°C for the zone-drawn/zone-annealed fiber[1] and the 3rd-step fiber prepared without vibration. The peak intensity is rapidly decreased with processes. The value for the 3rd-step fiber is slightly 0.023, which cannot be found in the literature. This indicates that the movements of amorphous chains are strongly inhibited.

CONCLUSION

1. The vibrating hot-drawing method was successfully applied to PET fiber and gave a high dynamic storage modulus at room temperature of 36 GPa.
2. The modulus of the 3rd-step fiber remains at a high level even at elevated temperatures, namely, 29 GPa at 100°C and 17 GPa at 200°C.
3. In spite of the relatively low draw ratio of 7.7, the high birefringence of 0.260 and orientation factor of amorphous chains of 0.749 were obtained.
4. From the high peak temperature of 155°C and the low peak height of 0.023 for the α_a dispersion peak in temperature–tan δ curves, it was found that the movements of amorphous chains are strongly inhibited.

Figure 3 Temperature dependence of dynamic storage modulus, E'; 1st-step fiber ($\triangle$), 2nd-step fiber ($\bigcirc$), 3rd-step fiber ($\square$), and the 3rd-step fiber prepared without vibration (-----).

REFERENCES

1. T. Kunugi, A. Suzuki, and M. Hashimoto, *J. Appl. Polym. Sci.*, **26**, 213 (1981); *ibid*, **26**, 1951 (1981).
2. J. C. Pereira and R. S. Porter, *J. Polym. Sci., Polym. Phys. Ed.*, **21**, 1147 (1983).
3. T. Kitao and T. Funabiki, *Kobunshi Ronbunshu*, **42**, 159 (1985).
4. K. J. Yoon, P. Desai, and A. S. Abhiraman, *J. Polym. Sci., Part B, Polym. Phys. Ed.*, **24**, 1665 (1986).
5. M. Ito, K. Tanaka, and T. Kanamoto, *J. Polym. Sci., Part B: Polym. Phys. Ed.*, **25**, 2127 (1987).
6. M. Amano and K. Nakagawa, *Polymer*, **27**, 1559 (1986); *ibid*, **28**, 263 (1987).
7. K. Itoyama, *J. Polym. Sci., Part C: Polym. Lett.*, **25**, 331 (1987).
8. M. Ito, K. Takahashi, and T. Kanamoto, *J. Appl. Polym. Sci.*, **40**, 1257 (1990).
9. S. Fakirov and M. Evstatiev, *Polymer*, **31**, 431 (1990).
10. S. D. Long and I. M. Ward, *J. Appl. Polym. Sci.*, **42**, 1911 (1991).
11. T. Kunugi, A. Suzuki, and T. Tsuiki, *Kobunshi Ronbunshu*, **48**, 703 (1991).
12. P. B. Rim and C. J. Nelson, *J. Appl. Polym. Sci.*, **42**, 1807 (1991).
13. U. Göschel, *Polymer*, **33**, 1881 (1992).
14. M. Ito, Y. Wakayama, and T. Kanamoto, *Sen-i Gakkaishi*, **48**, 569 (1992).
15. B. Huang, M. Ito, and T. Kanamoto, *Polymer*, **35**, 1329 (1994).
16. T. Kunugi, S. Oomori, and S. Mikami, *Polymer*, **29**, 814 (1988).
17. T. Kunugi, T. Kawasumi, and T. Ito, *J. Appl. Polym. Sci.*, **40**, 2101 (1990).
18. T. Kunugi and A. Suzuki, *ICFPR 1st International Conference on Frontiers of Polymer Research*, New Delhi, 1991, p. 116.
19. T. Kunugi and A. Suzuki, *2nd Pacific Polymer Conference*, Otsu, Japan, 1991, p. 339.
20. T. Kunugi, K. Chida, and A. Suzuki, *Polym. Prepr., Jpn.*, **39**(8), 2421 (1990).
21. T. Kunugi, H. Ishibashi, and A. Suzuki, *Sen-i Gakkai*, F-16 (1991).
22. A. Suzuki, K. Aihara, and T. Kunugi, *Kobunshi Ronbunshu*, **50**, 583 (1993).
23. R. De. P. Daubeny, C. W. Bunn, and C. J. Brawn, *Proc. R. Soc., Lond. Ser.*, **A226**, 531 (1954).
24. T. Kunugi, K. Shiratori, K. Uematsu, and M. Hashimoto, *Polymer*, **20**, 171 (1979).
25. V. B. Gupta, S. K. Sett, and D. D. Deorukhkar, *Polym. Commun.*, **30**, 341 (1989).
26. T. Kunugi, A. Suzuki, and T. Tsuiki, *4th SPSJ Intern. Polym. Conference*, Yokohama, Japan, **1C02**, 1992, p. 142.
27. A. J. DeVries, C. Bonnebat, and J. Beautemps, *J. Polym. Sci., Polym. Symp.*, **C58**, 109 (1977).
28. V. B. Gupta and S. Kumar, *J. Polym. Sci., Polym. Phys. Ed.*, **17**, 1307 (1979).
29. J. H. Dumbletom, *J. Polym. Sci., A-2*, **6**, 795 (1968).
30. H. M. Heuvel and R. Huisman, *J. Appl. Polym. Sci.*, **22**, 2229 (1978).